

Stability of Discrete Mechanical Systems Containing Negative Stiffness Components

Yun-Che Wang*

Department of Civil Engineering
National Cheng Kung University
Tainan, Taiwan 70101
E-mail: yunche@mail.ncku.edu.tw

Abstract

What is *negative stiffness*? Physically, when an elastic object is pressed, we expect it to resist by exerting a restoring force. This is called positive stiffness, which occurs when the deformation is in the same direction as the applied force, corresponding to a restoring force that returns the deformable body to its neutral position. A reversal of this force corresponds to negative stiffness (NS). Negative stiffness involves a reversal of the usual directional relationship between force and displacement in deformed objects. A caveat is that negative stiffness can also occur when force and deformation are along the same direction, but in this case the magnitude of the deformation would be large even under very small force. If we combine elements with positive and negative stiffness in a composite, it is possible to achieve stiffness greater than (or less than) that of any of the constituents. The effective stiffness may approach infinity, but it may be in a metastable state. This article summarizes the current development of the field and focuses on the stability of the NS discrete mechanical system. Furthermore, the equivalence among negative stiffness, pre-load and geometric nonlinearity is demonstrated through the discrete systems. Hence, no mystery in the field of negative-stiffness mechanics. Composites with inclusions of negative stiffness may be called exteoliberal because they are on the boundary of balance, or archidynamic because they are based on pre-stresses.

In this article, discrete mechanical systems are used to delineate the negative-stiffness phenomenon and its consequences. After the Introduction section, experimental evidence is presented in Section 2 since without the experimental findings there would be no need to study the negative-stiffness problem. In section 3, some remarks on stability theorems are given to facilitate understanding in the later sections. It is important to be familiar with the existing knowledge on the stability theorems in mechanics before we study the NS mechanical systems. In Sections 4, 5 and 6, discrete mechanical systems with or without NS components are discussed. Before the Conclusions and Outlook Section, some remarks on related issues and real-world applications are given in Section 7.

*Associate Professor

Contents

1	Introduction	3
2	Experimental evidence	4
3	Some remarks on stability analysis	5
3.1	General Considerations	6
3.2	Lyapunov's Theorems	8
4	One d.o.f. system: simple harmonic oscillator	9
5	One d.o.f. negative-stiffness system	11
6	Discrete viscoelastic composites with the negative stiffness element	13
7	Some remarks on related issues and real-world applications	18
7.1	Negative stiffness vs. negative Poisson's ratio (or called auxetic materials)	18
7.2	Negative stiffness does not violate thermodynamic laws	18
7.3	Negative stiffness vs. negative permittivity	18
7.4	Real-world applications	18
8	Conclusions and outlook	19
9	Acknowledgments	19

1 Introduction

In mechanics, stiffness refers to the ratio of the generalized force to the generalized displacement. For a spring the stiffness is the ratio of the force to the displacement: the usual spring constant k . For a three-dimensional solid viewed as a continuum in the context of elasticity theory [42], the measure of stiffness is the ratio of the stress (force per area) to the strain (displacement per length), referred to as a modulus. For example, Young's modulus and the shear modulus are used for axial and torsional properties, respectively. Modulus is a continuum property independent of the geometry and size of the material.

Negative stiffness may be obtained through postbuckling processes, as indicative of the non-monotonic load displacement curves. Snap-through buckling may occur when under load control. For materials undergoing solid-solid phase transformation, snap through also occurs on the atomic scale in materials such as ferroelastic solids which exhibit a solid to solid phase transformation (Puglisi and Truskinovsky 2000) [36]. Indirect experimental evidence of negative shear modulus is found in the banding instability which occurs in compressed foams (Rosakis *et al.* 1993) [37]. In ferroelastic, ferroelectric and ferromagnetic materials (Salje 1990) [38] the bands, called domains, occur below a transition temperature T_c . In a ferroelastic the free energy in the Landau theory has a relative maximum, corresponding to unstable equilibrium, below its transformation temperature T_c (Falk 1980) [10]. Small particles may be single domains, owing to surface energy; domain size can be from nm to cm scale depending on the material. A negative stiffness material may be represented by an energy vs. deformation diagram in which there are at least two relative minima or energy wells. Negative stiffness was directly observed experimentally in tetrakaidecahedral single cell models of foam materials, in compression under displacement control constraint (Rosakis *et al.* 1993) [37]. The concept of composites with negative stiffness is supported by experimental study of a constrained, lumped one-dimensional model system involving a single buckled tube as a negative stiffness element (Lakes 2001) [22]. Negative stiffness can be achieved in pre-stressed elastic systems including tubes or structures following buckling, in pre-loaded lattices, and in ferroelastic materials just below their phase transformation temperature. In ferroelastics one may visualize the negative stiffness in the context of the Landau energy theory for transformations in which stiffness is the derivative of energy with respect to deformation.

When composites consisting of positive- and negative-stiffness phases, the overall properties of the composites may be extreme. The rationale for expecting extreme behavior in systems with one negative stiffness phase can be understood by considering the following thought experiments based on simple mechanical spring models. For a parallel elastic system, $E_c = E_1 V_1 + E_2 V_2$, where E_c , E_1 , and E_2 refer to the Young's modulus of the composite, phase 1, and phase 2, respectively. V_1 and V_2 refer to the volume fraction of phase 1 and phase 2 with $V_1 + V_2 = 1$. The parallel elastic system has bonded phases which undergo the same strain and is known as the Voigt model (Paul 1960) [35]. If we have parallel springs of spring constant k , then $k_c = k_1 + k_2$. Similarly, for a series system of springs, $k_c = 1/(k_1^{-1} + k_2^{-1})$. The system of springs in series is analogous to the Reuss model in composites (Paul 1960) [35]. In the series system, we can express the compliance $j = 1/k$ as $j_c = j_1 + j_2$. If one stiffness is negative, the corresponding compliance is negative. We can sum a positive and negative compliance to obtain a zero compliance and hence an infinite stiffness. Therefore, extreme, and even singular stiffness is possible in heterogeneous systems with a negative stiffness constituent. However, a negative stiffness element by itself is unstable, and the series model also is unstable. If systems containing negative stiffness can be made stable, they can be useful as a result of the unexpected large values of their physical properties.

Not only can a negative stiffness inclusion magnify the overall mechanical properties of a composite, but also its coupled field properties, such as thermal expansion coefficient, piezoelectric constants, pyroelectric coefficients and even overall electric permittivity. Particulate composites with negative stiffness inclusions in a viscoelastic matrix are shown to have higher thermal expansion than that of either constituent and exceeding conventional bounds. It is also shown theoretically that other extreme linear coupled field properties including piezoelectricity and pyroelectricity occur in layer- and fiber-type piezoelectric composites, due to negative inclusion stiffness effects. The causal mechanism is a greater deformation in and near the inclusions than

the composite as a whole. A block of negative stiffness material is unstable, but negative stiffness inclusions in a composite can be stabilized by the surrounding matrix and can give rise to extreme viscoelastic effects in lumped and distributed composites. In contrast to prior proposed composites with unbounded thermal expansion, neither the assumptions of void spaces nor slip interfaces are required in the present analysis.

A material with negative stiffness is in unstable equilibrium, because the material has a higher positive stored energy at equilibrium, compared to neighboring possible equilibrium configurations. A material with negative stiffness can be stable if it is constrained. For example, the buckled ruler is an example of such a stabilizing constraint. Also, a buckled rubber tube has a negative stiffness component (Lakes 2001) [22], and experimentally reveals a large peak in the mechanical damping, consistent with the prediction of the Reuss model with one phase having negative stiffness. The stability of mechanical systems with negative stiffness inclusions is intriguing. A complete and definite stability criterion for an elastic solid is still in question and subject to debate. A bulk solid of negative stiffness materials is unquestionably unstable, but if all of its boundaries are fully constrained in displacement control, it can be stable, in which stability requires shear modulus (G) and Poisson's ratio (ν) to be $G > 0$ and $-\infty < \nu < 0.5$ or $1 < \nu < \infty$ (Bramble and Payne, 1963) [4]. Since Young's modulus is $E = 2G(1 + \nu)$ for isotropic homogeneous materials, the Young's modulus can legitimately be negative for constrained solids. Furthermore, if the condition of strong ellipticity, $G > 0$ and $\nu < 0.5$ or $\nu > 1$, is satisfied, isotropic and homogeneous materials can have negative bulk and Young's modulus without losing uniqueness in their elasticity solutions (Knowles and Sternberg, 1978) [19] under no restrictions on boundary condition. Also, it implies real waves can propagate in the media. For traction boundary value problems, satisfying the strong ellipticity condition does not imply stability (Gurtin 1981) [?]. However, these criteria are only valid for homogeneous materials comprised of a single constituent. There is little, almost no, research on stability of composites in the literature. Lakes and Drugan (2002) [25] demonstrated that Reuss-type composites with negative stiffness inclusions are unstable, based on an energy argument in the linear elasticity context. A negative stiffness lumped element (a structure) may be stabilized by a hard constraint.

2 Experimental evidence

Material properties, stiffness and damping ($\tan \delta$; δ is the phase between stress and strain) as a function of temperature of a particulate VO₂-Sn composite with 1% by volume of inclusions are shown in Figure 1. The theoretical predictions are shown in Figure 1 (a), and experimental data are shown in Figure 1 (b). Although the concentration of inclusions is dilute, large anomalies are observed in the mechanical damping, $\tan \delta$ as well as in the stiffness. For comparison, $\tan \delta$ of pure Sn is 0.019 and varies little with temperature as shown. The sharp dependence on temperature is attributed to the fact the inclusions are much stiffer than the matrix (away from the transition temperature) and can only balance the matrix stiffness near the transition. The peaks observed in the present 1% VO₂ composite are larger than in 100% VO₂, which had a peak (Zhang *et al.* 1995) 0.04 to 0.05 in $\tan \delta$ and a dip of 8% in stiffness at the transition. In the composite, there is interplay between constituents of positive and negative stiffness; by contrast 100% VO₂ has positive stiffness at all temperatures due to the formation of domains. Analysis based on an assumption of negative stiffness inclusions predicts a sharp peak in $\tan \delta$ and a modulus anomaly as shown in Figure 1(a).

Hashin-Shtrikman (1963) [13] formulas provide a means of estimating the bounds of effective shear and bulk modulus for a two phase composite. As for the shear and bulk modulus of each phase as input to Eq. (1), the lower bounds for the elastic shear modulus G_L and bulk modulus K_L of a composite are:

$$G_L = G_2 + \frac{V_1}{\frac{1}{G_1 - G_2} + \frac{6(K_2 + 2G_2)V_2}{5(3K_2 + 4G_2)G_2}}, \quad (1)$$

$$K_L = K_2 + \frac{V_1(K_1 - K_2)(3K_2 + 4G_2)}{3K_2 + 4G_2 + 3(K_1 - K_2)V_2}, \quad (2)$$

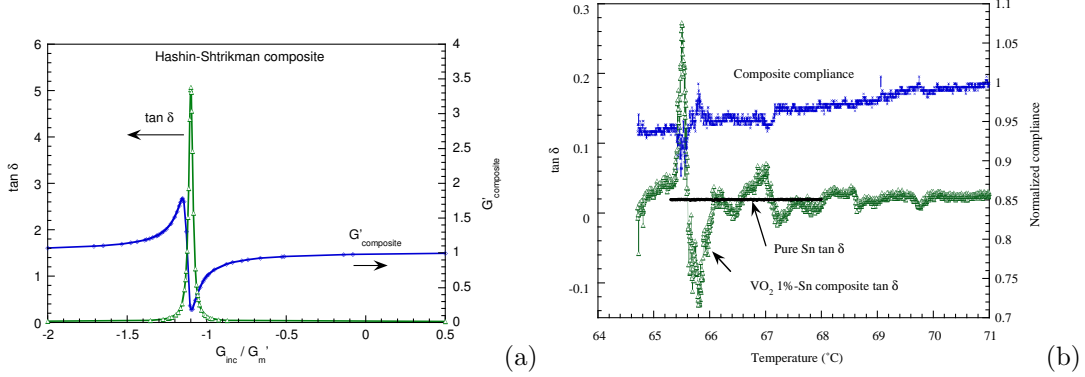


Figure 1: (a) Theoretical shear modulus G' (real part) and mechanical damping $\tan \delta$ vs. inclusion shear modulus G_1 normalized to matrix shear modulus G_2 , of Hashin-Shtrikman composite containing 1% of spherical particulate inclusions by volume. (b) Experimental results on the VO_2 -Sn composite [24].

in which K_1 and K_2 , G_1 and G_2 , and V_1 and V_2 are the bulk modulus, shear modulus and volume fraction of phases 1, and 2, respectively. If $G_1 > G_2$, then G_L represents the lower bound on the shear modulus. Interchanging the subscripts 1 and 2 results in the upper bound G_U for the shear modulus. The bounds for isotropic composites are attainable. The Hashin-Shtrikman formula for the bulk modulus, Eq.(2), is attained exactly by a coated sphere morphology. The 'lower' composite corresponds to the case of stiff spheres coated with a compliant layer. The shear modulus of the coated sphere morphology approximates the corresponding Hashin-Shtrikman formula, Eq.(1). Exact attainment of Eq.(1), however, is possible via a laminate morphology (Milton 1986) [33] as shown by Milton.

For viscoelastic materials, the moduli become complex following the elastic-viscoelastic correspondence principle (Christensen, 1982) [6]. When the inclusion phase 1 has a negative shear modulus about -1.1 of the matrix modulus, composite behavior (Lakes 2002a) [23] is predicted to exhibit a large peak in damping, $\tan \delta$, and an anomaly in stiffness. As an illustration of the concept, Figure 1 shows representative behavior vs. inclusion stiffness based on composite theory with isotropic inclusions and matrix. The abscissa is normalized inclusion stiffness, which is tuned indirectly via temperature in the experiments. If inclusion concentration is increased or matrix damping is reduced, theory allows the composite to have negative stiffness and $\tan \delta$. The theory is simplistic in that inclusion anisotropy and heterogeneity of their environment is ignored.

Recent experimental results show that the effective stiffness of the BaTiO_3 -Sn composites can become larger than that of diamond due to the negative-stiffness effects, as shown in Figure 2(a). As can be seen, effective damping is also enhanced during the phase transition of the barium titanate at the transformation temperature. In Figure 2(b), the mechanical behavior of the composites after several thermal cycles is shown. The stiffness and damping anomalies diminish with thermal cycles. The mechanisms of the cycle-dependent phenomenon are currently a research topic with intensive activities.

3 Some remarks on stability analysis

Ever since Newton (1677) formulated his laws of mechanics, the stability of a dynamical system has concerned most of his followers. At the end of 19th century, King Oscar of Sweden offered a prize to the first person who could show once for all that our solar system, including the sun, planets, and other small objects, is stable (Stewart 1997). Henri Poincare (1854-1912) took the chance, studied a simplified problem (i.e. the three body problem), and won the prize, although he did not completely solve the problem. Richard

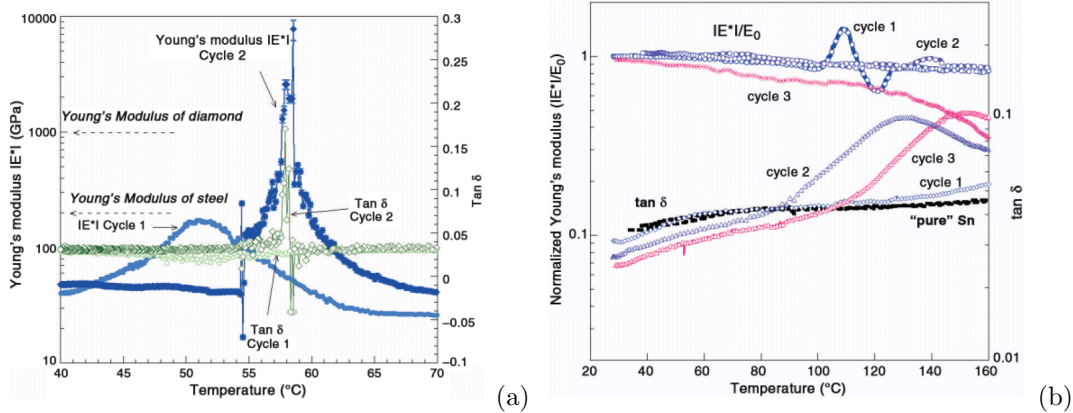


Figure 2: (a) Stiffness greater than diamond. (b) Cycle-dependent responses [16].

Bellman pointed out that stability is a ‘much overburdened word with an unstabilized definition’ (Bellman 1953) [2]. Lyapunov (1892, 1897) [29] established fundamental stability theory, believed to be ‘universal’ valid across different platforms. In the beginning of the 20th century, mathematicians started realizing that the fundamental problem of stability relies on the definition of measures in analysis (Knops and Wilkes) [20]. Since then, the stability analysis has become very mathematical.

The stability of a system can be demonstrated and understood through the following three pictures, Figure 3. For $\lambda > 0$, the system is stable; $\lambda = 0$, the system reaches its stability limit (sometimes the stability is this case is called neutral); $\lambda < 0$, the system is unstable. Here the symbol λ should be distinguished from eigenvalues. The variable λ can be considered as the degree of stability. In general, the problems in stability analysis can be classified into two categories: one is time-invariant (autonomous), and the other is time-dependent (non-autonomous) problems. Mathematically, the goal of the stability analysis is to find the regions of control parameters such that the solutions of the differential equations corresponding to the mechanical (or electrical) system will not be unbounded as time approaches infinity. The control parameters are usually the magnitude of loading, the direction of loading, or driving frequencies.

A stability analysis can usually be done via two different approaches. One approach is to investigate the energy landscape of the system. This approach is only suitable for systems without energy dissipation. A region with a concave up energy profile, that is, the second derivative of the energy function is greater than zero, indicates that the system is locally stable around the equilibrium position (Leipholz 1987) [28]. An alternative method is to examine the eigenvalues of the perturbed dynamical system in the context of Lyapunov’s stability theorem (Leipholz 1987, Marsden and Ratiu 1994) [28] [30]. This approach allows one to accommodate effects of dissipation, stored energy, and input power. Lyapunov’s indirect method will be adopted here for a system with non-conservative components, as shown in Figure 3(b).

3.1 General Considerations

Lyapunov’s indirect method often is called the Routh-Hurwitz criterion in electrical engineering (Marsden and Ratiu 1994, Merkin 1997) [30] [32]. This type of stability analysis is used to analyze electronic circuits that contain elements such as capacitors which store energy, and amplifiers. The method predicts the stability of a discrete autonomous dynamical system, governed by

$$\dot{\mathbf{x}} = \mathbf{X}(\mathbf{x}), \quad \text{or} \quad (3)$$

$$\dot{x}_i = X_i(x_1, x_2, \dots, x_m), \quad i = 1, 2, \dots, m. \quad (4)$$

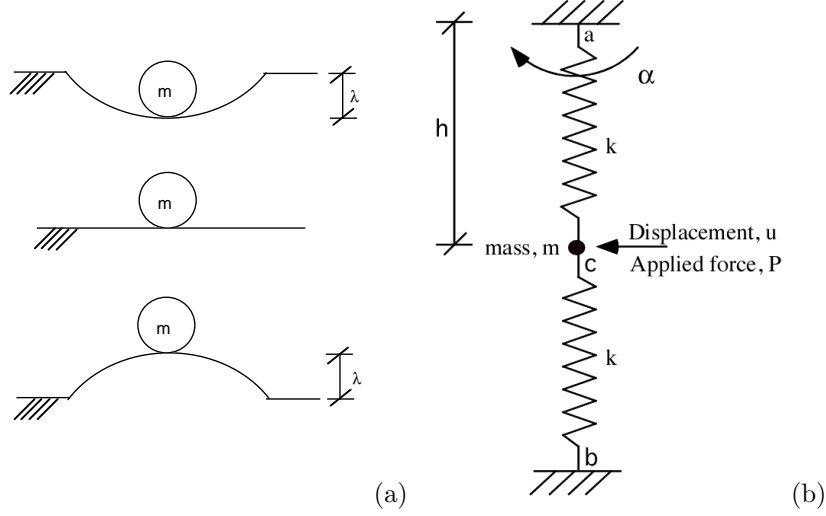


Figure 3: (a) Visualization of stability. (b) A spring system that can exhibit positive or negative stiffness depending on the pre-load. The symbol k represents the spring constant, the angle α the generalized coordinate describing the motion of the springs, and f^0 (not shown) the initial force in each spring.

where \mathbf{X} is a column-vector function of \mathbf{x} , $\mathbf{x} = \mathbf{x}(t)$ is a column-vector function of time, and the super-dot denotes differentiation with respect to time. The symbol m denotes the number of state variables. In the following, we write down explicit expressions of \mathbf{x} and \mathbf{X} for the Hamiltonian systems.

For a Hamiltonian with $H = H(q_k, p_k)$, where $k = 1, 2, \dots, n$, where n is the total number of degrees of freedom, and x and X can be constructed as follows.

$$x_k = q_k, x_{n+k} = p_k, \quad \text{and} \quad (5)$$

$$X_k = \partial H / \partial p_k, X_{n+k} = -\partial H / \partial q_{n+k} \quad (6)$$

where

$$\dot{q}_k = \frac{\partial H}{\partial p_k}, \quad \text{and} \quad \dot{p}_k = -\frac{\partial H}{\partial q_k}, \quad (7)$$

q_k and p_k are generalized coordinates and generalized momenta, respectively. It is noted that $m = 2n$.

If the systems are non-Hamiltonian, such as dissipative systems, one still can construct the governing equations into the form, as Equation (4), through Newton's second law and the state-space technique, which in essence reduces higher order differential equations to a system of first order differential equations. In this case, the physical meaning of the variables will be somewhat obscure. Also, the dimension of Equation (4), m , is not necessary to be an even number. However, the methodology for stability analysis is unchanged.

A general strategy of investigating the stability of Eq. (3) is to assume the solution to be $\mathbf{x} = \mathbf{x}_0 + \delta\mathbf{x}$, where x_0 is the equilibrium solution of the system around some origin. Then, one can derive the perturbed equations, governing $\delta\mathbf{x}$. However, one can show that this could be done via the calculus of variations [28]. Using the calculus of variations, the perturbation of the dynamical system can be readily written down to a first order, as follows.

$$\frac{d}{dt}(\delta\mathbf{x}) = \mathbf{J}|_{\mathbf{x}_e} \cdot \delta\mathbf{x}, \quad (8)$$

where the Jacobian matrix $\mathbf{J} = \partial\mathbf{X}/\partial\mathbf{x}$, or $J_{ij} = \partial X_i / \partial x_j$. The subscript \mathbf{x}_e indicates that the matrix, \mathbf{J} , is evaluated at the equilibrium point ($d\mathbf{x}/dt = 0$), $\mathbf{x} = \mathbf{x}_e$, where $\mathbf{X}(\mathbf{x}_e) = 0$. It is understood that

any conclusions derived from Eq.(8) will be classified as infinitesimal stability. For obtaining the stability conditions in the large, one needs to go beyond linearized systems, and use the Lyapunov direct theorem.

It is noted that for static problems, one can derive stability conditions without going through above-mentioned concepts. Due to L. Euler, one can use a completely different idea to investigate other equilibrium configurations of a static problem, such as static buckling. The idea is first to assume that another equilibrium configuration exists. Then, one can derive the corresponding governing equations with some buckling parameter included. Finally, solve some eigen problems to determine the buckling parameter. The main drawback of this method is that one needs to be able to construct the configuration after buckling first. The method is only good for time-independent problems. However, one can see that Euler's method and the method for dynamical systems are at the two ends of the spectrum for attacking stability problem in mathematical physics. The first is suitable for time-independent, spatial continuous problems, and the latter for time-dependent, spatial continuous ones. We remark that although Euler's method cannot be directly extended to dynamical problems, one is able to extract time information during buckling with perturbation techniques.

3.2 Lyapunov's Theorems

The Soviet mathematician A. M. Lyapunov [31] rigorously formulated the stability theorems connecting the concept of energy considerations and that of equilibria of differential equations, which are coined the Lyapunov indirect (first) theorem and Lyapunov direct (second) theorem. In essence, the Lyapunov indirect theorem is the same as the Routh-Hurwitz criterion for linearized dynamical systems, but the latter provides a unique way to determine the stability without calculating the eigenvalues of the systems directly. Lyapunov's direct theorem determines the stability of nonlinear or even non-autonomous dynamical systems with the concept of non-infinitesimal stability. However, constructing the so-called Lyapunov function is not trivial. The proof of the theorems can be found in Lyapunov's original papers, collected in [29].

Theorem 1 (Lyapunov indirect theorem) *If all roots of the characteristic equation (e.g. Eq.(11)) of a first approximation of a dynamical system have negative real parts, then irrespective of terms of higher than one, the unperturbed motion is asymptotically stable.*

Theorem 2 (Lyapunov direct theorem) *If for the differential equations of a perturbed motion of a dynamical system we can find a definite function V such that by virtue of the given equations its derivative is either identically equal to zero or is semi-definite with the opposite sign of V , then the unperturbed motion is stable. If V is a definite function with the opposite sign of V , then the unperturbed motion is asymptotically stable.*

Following Lyapunov's indirect method, if all the roots of the characteristic equation of the matrix \mathbf{J} of the perturbed system in Eq.(8) have negative real parts, then the unperturbed system, Eq.(3) is asymptotically stable (Merkin 1997) [32]. The \mathbf{J} matrix is called Jacobian, and can be calculated as follows.

$$J_{ij} = \frac{\partial \mathbf{X}_i}{\partial \mathbf{x}_j}. \quad (9)$$

The characteristic equation of the system is defined as follows.

$$\det(\mathbf{J} - \lambda \mathbf{I}) = 0, \quad \text{or} \quad (10)$$

$$a_0 + a_1 \lambda + a_2 \lambda^2 + a_3 \lambda^3 + \dots + a_n \lambda^n = 0, \quad (11)$$

Here the coefficient a_i , $i = 1, 2, 3, \dots, n$ are composed of the elements in \mathbf{J} . Eq.(10) or (11) is called the characteristic equation of the linearized system in Eq.(8).

When the real parts of the eigenvalues are zero, we need to investigate the imaginary part of the eigenvalues or the reduction in the eigenspace of the system. In this case the system will be stable when the imaginary part is nonzero (Meirovitch 1970) [31]. Strogatz (1994) [41] points out that the stability of a dynamical system with zero real part in its eigenvalues is weak albeit stable. When all eigenvalues have negative real parts, the degree of stability can be understood as the distance between the imaginary axis and the closest eigenvalue in the complex plane for all the eigenvalues of the system (Leipholz, 1987) [28]. Furthermore, the eigenvalue (λ), which has the smallest $|\Re(\lambda)|$, is responsible for the rate of decay (for $\Re(\lambda) < 0$) or growth (for $\Re(\lambda) > 0$) of vibration amplitudes in the system's normal modes.

A stable and convergent response is called asymptotically stable. It is understood that the Lyapunov's direct theorems are only sufficient conditions for stability, which means if one cannot find a Lyapunov function, it does not mean that the system is unstable. As for Lyapunov's indirect theorem, one needs special treatments for the case when some or all of the real parts of the eigenvalues are zero (Leipholz, 1980) [27]. However, for linear systems or linearized non-linear systems with the assumption of small perturbation, zero real parts for all eigenvalues indicate that the system is stable when the corresponding imaginary parts do not vanish (Meirovitch 1970) [31]. In other words, the multiplicity and nullity of the Jacobian matrix are the same so that there is no reduction in its eigenspace.

For the stability analysis with the first order approximation, the degree of stability of a system can be calculated from the eigenvalues of the system's Jacobian matrix if the system is autonomous. By definition (Meirovitch 1970, p.174) [31], if the vector \mathbf{X} in Eq.(9) does not explicitly depend on time, i.e. $\mathbf{X} = \mathbf{X}(x_1, x_2, \dots, x_n)$, the system is called to be autonomous. A non-autonomous system is in general non-conservative. The non-conservative origins could be due to internal properties of the system or boundary conditions. The idea is followed by the Lyapunov's indirect theorem. The negative real part of all eigenvalues ensures the stability of the system. The smallest absolute real part of all eigenvalues is defined as the degree of stability. Physically, it is understood this smallest number controls the time for the system damping out. The smaller the degree of stability is, the more time the system needs to damp out. For the pure elastic cases, the degree of stability is zero, which can be understood that the system is at the stability limit. For non-autonomous or non-linear stability analysis, one can further define the global degree of stability. We remark that the conventional energy method is not suitable for the stability analysis of a dissipative system due to the changing in the energy landscape with respect to time (since mechanical energy is not conserved in such systems). According to Lyapunov's indirect theorem for stability, at an equilibrium point, if \mathbf{J} contains eigenvalues with no positive real parts, the system is stable infinitesimally around the equilibrium point.

For historical reasons, we mention that directly solving all eigenvalues of the \mathbf{J} matrix is not the only way to identify the stability of a system. Routh-Hurwitz criteria provide the same stability information by using only the algebraic relations between coefficients of the characteristic equation of the \mathbf{J} matrix. Dorf (1992) [8] uses an iteration scheme to discuss the stability of the system, which essentially predicts the same result as Routh-Hurwitz criteria. In our study, we exclusively analyze the eigenvalues with sufficient computational power.

4 One d.o.f. system: simple harmonic oscillator

This Section serves two purposes. One is to look into the familiar mechanical system so that we can use our physical intuition to justify mathematical results, and the other to demonstrate the extended energy method [27] to prove the stability of the system. No negative-stiffness in this example is assumed. However,

it is noted that dynamic negative stiffness commonly occurs when driving frequency passes through resonance [45]. And, this phenomenon is stable due to the out-of-phase relationship between input and output. For the single degree of freedom (d. o. f.) system, which consists of a Hookean spring (k), a point mass (m) and external load (F), by Newton's second law, the equation of motion is

$$m\ddot{u} + ku = F, \quad (12)$$

where m is the mass, k the stiffness, $u = u(t)$ the displacement, and $F = F(t)$ the external driving force. A superdot indicates the derivative with respect to time. The solution of the equation of motion in the time domain is as follows. Assume $F = P + A \cos \Omega t$, and P and A are constants.

$$u = u^h + u^p, \quad (13)$$

where the homogeneous solution $u^h = C_1 e^{\lambda_1 t} + C_2 e^{\lambda_2 t}$, where $\lambda_{1,2} = \pm i\omega$ and $\omega^2 = k/m$, and C_1 and C_2 are constants to be determined by initial conditions. As for the particular solutions, u^p , one can express them as follows.

$$u^p = \frac{P}{k} + \frac{A \cos \omega t}{-m\Omega^2 + k}, \quad \text{when } \Omega \neq \omega. \quad (14)$$

$$u^p = \frac{P}{k} + \frac{t}{2\Omega} A \sin \Omega t, \quad \text{when } \Omega = \omega. \quad (15)$$

It is clear to see that instability occurs only when $\Omega = \omega$, due to time-growing behavior in its particular solution. Therefore, from this time domain analysis, the stability criterion is that the system is stable when $\Omega \neq \omega$. This stability criterion can also be obtained through analysis in the frequency domain. Applying a Fourier transform on Eq.(12), one converts the governing equation into an algebraic equation, as follows.

$$\frac{\tilde{u}}{\tilde{F}} = \frac{1}{-m\omega^2 + k}. \quad (16)$$

The instability of the system occurs only when $\omega^2 = k/m$, which is consistent with previous results. Furthermore, the results indicate that the system is internally stable when $F = 0$ and $k/m > 0$. Moreover, the system is also stable when $k < 0$ and $m < 0$. For $k/m < 0$, there are no oscillatory solutions for the system, only real exponential ones. Hence, it is internally unstable.

The internal stability is the stability of a system under no external forcing. However, in some cases, it is important to investigate a dynamical system with time variables explicitly (i.e. non-autonomous systems), such as flutter analysis. A general method for attacking this problem is to consider the time variable as an ordinary spatial variable. However, by doing so, the Lyapunov indirect method will not be suitable for stability analysis since it is local. The Lyapunov direct method can be applied, but stability must be checked at all times in the time domain. Here, we adopt the extended energy method for demonstration.

Alternatively, one can rigorously derive the stability criteria of a mechanical system by using the so-called extended energy method [27]. Using the system depicted in Eq.(12) as an example, first, we re-write the equation of motion for the system as follows.

$$\ddot{q} + \omega^2 q = \frac{A}{m} \cos \Omega t. \quad (17)$$

where $q = q(t)$ is the generalized coordinate, ω^2 the ratio of k to m , and Ω the driving frequency. $q(t)$ is different from $u(t)$ in that the latter contains the contribution from the dead load P . The total energy of the system can be calculated as follows.

$$E = \int_0^t (\ddot{q} + \omega^2 q - \frac{A}{m} \cos \Omega t) \dot{q} dt - \frac{1}{2} \dot{q}^2 + \frac{1}{2} \omega^2 q^2 - \int_0^t (\frac{A}{m} \cos \Omega t) \dot{q} dt. \quad (18)$$

It is clear to see that the energy is not a first integral of the system. From (18), it is understood that the Hamiltonian and non-conservative force can be written as follows.

$$H = \frac{1}{2} p^2 + \frac{1}{2} \omega^2 q^2, \text{ and} \quad (19)$$

$$N = \frac{A}{m} \cos \Omega t. \quad (20)$$

Here $p = \dot{q}$. Define $\phi = \phi(q, \lambda, \Omega) = dE$, and, for $E = E(q, p, \Omega)$, the explicit representations of ϕ and $d\phi$ are as follows.

$$\phi = \frac{\partial H}{\partial q} - N + G = 0, G = \frac{\partial H}{\partial p} p. \quad (21)$$

$$d\phi = \frac{\partial \phi}{\partial q} dq + \frac{\partial \phi}{\partial \lambda} d\lambda + \frac{\partial \phi}{\partial \Omega} d\Omega = 0. \quad (22)$$

or

$$\left(\frac{\partial^2 H}{\partial q^2} - \frac{\partial N}{\partial q} + \frac{\partial G}{\partial q}\right) dq + \left(\frac{\partial G}{\partial \lambda} - \frac{\partial N}{\partial \lambda}\right) d\lambda + \left(\frac{\partial^2 H}{\partial \Omega \partial q} - \frac{\partial N}{\partial \Omega}\right) d\Omega = 0. \quad (23)$$

Here λ is the characteristic frequency of the system. In the present case, λ is chosen to be Ω , and Ω is the control parameter in the stability analysis, which means the results of the stability analysis will indicate a specific value or region for Ω to make the system unstable. In order to calculate ϕ in terms of λ explicitly, we assume the solution for q as follows.

$$q = B \cos(\lambda t + \Phi) = B \cos(\Omega t + \Phi) \quad (24)$$

Here B and Φ are to be determined. Consequently, p can be found as follows.

$$p = \dot{q} = -B\Omega \sin(\Omega t + \Phi) = -\Omega \sqrt{B^2 - q^2}. \quad (25)$$

Thus, the G in Eq.(12) can be calculated as follows.

$$G = p \frac{dp}{dq} = (-\Omega \sqrt{B^2 - q^2}) \left(-\Omega \frac{1}{2} \frac{1}{\sqrt{B^2 - q^2}} (-2q)\right) = \Omega^2 q. \quad (26)$$

When the instability occurs, $dq/d = \infty$. The instability occurs when the following equation is satisfied.

$$\frac{\partial^2 H}{\partial q^2} - \frac{\partial N}{\partial q} + \frac{\partial G}{\partial q} = 0, \quad \text{or} \quad \omega^2 - \Omega^2 = 0. \quad (27)$$

Clearly, (27) suggests the system is unstable only when the driving frequency is equal to the natural frequency of the system, as expected.

The importance of the above results is the rigorous proof of the stability of the simple harmonic oscillator. It is stable everywhere in the frequency domain except at the resonance. Hence, dynamic negative stiffness is stable. However, at resonance, the simple harmonic system can be stabilized in the sense that no unbounded responses occur, if damping elements are included. Without driving force, the system is internally stable when both mass and stiffness are positive or negative. Negative mass has been an interesting research subject [14].

5 One d.o.f. negative-stiffness system

To demonstrate the relation between Lyapunov's indirect method and known cases of stability and instability, the spring system with a negative stiffness element (shown in Figure 3(b)) is analyzed here. The negative stiffness arises from a compressive pre-load in the springs. The equation of motion for the system is

$$m\ddot{u} + 2 \left[kh \left(\frac{1}{\cos \alpha} - 1 \right) + f^0 \right] \sin \alpha = P, \quad (28)$$

where $u = u(t)$, and $\alpha = \alpha(t)$. The symbol f^0 represents the pre-load inside both the ac and bc springs and should be distinguished from the applied force, P . If we replace the displacement u by the generalized coordinate α , we can express the equation of motion as

$$(mh \sec^2 \alpha) \ddot{\alpha} + (2mh \sec^2 \alpha \tan \alpha) \dot{\alpha}^2 + 2kh \tan \alpha - 2kh \sin \alpha + 2f^0 \sin \alpha = P. \quad (29)$$

To investigate the stability around $\alpha \ll 1$ (corresponding to a vertical position of the springs) and $d\alpha/dt \ll 1$ with $P = 0$, Eq.(29) can be further simplified:

$$\ddot{\alpha} + \frac{2f^0}{mh} \alpha = 0. \quad (30)$$

To obtain the general form of the equation of motion for a dynamical system, as in Eq.(3), the standard method, which is called the state-space technique for reducing higher order ordinary differential equations to lower order ones is used so that Eq.(30) can be rewritten as follows (Meirovitch 1970) [31]. The first step in using Lyapunov's indirect method to investigate the stability is to change a higher order differential equation to a system of first-order differential equations:

$$\begin{pmatrix} \dot{\alpha} \\ \dot{q} \end{pmatrix} = \begin{bmatrix} 0 & 1 \\ -\frac{2f^0}{mh} & 0 \end{bmatrix} \begin{pmatrix} \alpha \\ q \end{pmatrix}. \quad (31)$$

where $q = d\alpha/dt$. Near the equilibrium point, $\alpha = 0$ and $q = 0$, and \mathbf{J} is

$$\mathbf{J}_{\mathbf{x}_e} = \begin{bmatrix} 0 & 1 \\ -\frac{2f^0}{mh} & 0 \end{bmatrix}. \quad (32)$$

The characteristic equation of \mathbf{J} is

$$\lambda^2 + \frac{2f^0}{mh} = 0 \quad (33)$$

and hence,

$$\lambda_1 = \sqrt{\frac{2|f^0|}{mh}} + i0, \quad (34)$$

$$\lambda_2 = -\sqrt{\frac{2|f^0|}{mh}} + i0.. \quad (35)$$

for $f^0 < 0$ (pre-compressed), and

$$\lambda_1 = 0 + i\sqrt{\frac{2|f^0|}{mh}}, \quad (36)$$

$$\lambda_2 = 0 - i\sqrt{\frac{2|f^0|}{mh}}.. \quad (37)$$

for $f^0 > 0$ (pre-stretched), where λ represents the eigenvalues of \mathbf{J} . We conclude that the system is unstable when $f^0 < 0$, because $\Re(\lambda_1) > 0$ in Eq.(34), and is stable when $f^0 > 0$, because $\Re(\lambda_1) = \Re(\lambda_2) = 0$ in Eqs.(36) and (37) with nonzero imaginary parts. Note that the magnitude of the eigenvalues will be extremely large when the mass m approaches zero. These eigenvalues with large positive real part cause the system to diverge rapidly from unstable equilibrium when the mass is small. Physically, it is understood that the system is locally stable in a pre-stretched state (that is, tensile pre-load) like a guitar string, but cannot be locally stable in a pre-compressed state (that is, a compressional pre-load).

If we perform the stability analysis by the energy method (Iesan 1989) [15], the total energy and its second derivative can be expressed as:

$$U = kh^2(\sec \alpha - 1)^2 + 2f^0 h(\sec \alpha - 1), \quad (38)$$

$$\left. \frac{\partial^2 U}{\partial \alpha^2} \right|_{\alpha=0} = 2f^0 h. \quad (39)$$

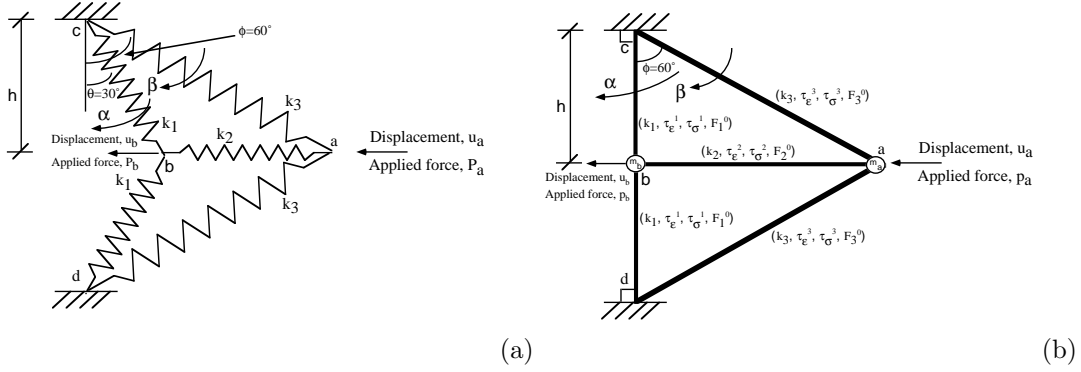


Figure 4: (a) Two-dimensional spring system, undeformed configuration. (b) The critical configuration for the extreme properties [44].

Clearly, if $f^0 > 0$, U is always greater than 0, and the $U(\alpha)$ is concave up around $\alpha = 0$, that is, $x = 0$, the equilibrium point, which indicates that the system is stable; if $f^0 < 0$, the system is unstable. We see that the results of the stability analysis can be obtained from both methods, and a spring system with a compressional pre-load is unstable around the equilibrium point, $\alpha = 0$, consistent with our physical intuition. The pre-compressed two-spring structure expresses the instability of unconstrained negative-stiffness materials. The stability analysis performed here is crucial for understanding the later analysis for extreme stiffness phenomena. In the following we will embed a negative stiffness element into other positive stiffness elements and investigate the system's unusual mechanical properties. Then, the stability analysis of a simplified spring model will be discussed.

6 Discrete viscoelastic composites with the negative stiffness element

A discrete model is shown in Figure 4 to include the effects of pre-load in the context of full geometrical nonlinearity. The goal is to explore interesting phenomena in the vicinity of the snap-through of springs bc and bd . The static or dynamic equations of motion have to be expressed with respect to the deformed configuration in order to fulfill the requirement of geometrical nonlinear analysis. Governing equations of the model for the purely elastic case with the consideration of geometric nonlinearity (as shown in Figure 4(a)) are as follows. For the mathematical system of the viscoelastic case for Figure 4(b), the reader is referred to Reference [44].

We let the angles α and β represent the change of θ and ϕ after the deformation as shown in Figure 4, and interpret α and β as generalized coordinates. The change of the lengths of the springs, denoted by Δ , can be related to the generalized coordinates as:

$$\Delta_1 = \frac{h}{\cos(\theta - \alpha)} - \frac{h}{\cos \theta}, \quad (40)$$

$$\Delta_2 = [h \tan(\phi - \beta) - h \tan(\theta - \alpha)] - (h \tan \phi - h \tan \theta), \quad (41)$$

$$\Delta_3 = \frac{h}{\cos(\phi - \beta)} - \frac{h}{\cos \phi}. \quad (42)$$

Once the relationship between the deformation of springs and the generalized coordinates is found, the total potential energy of the spring system, including the contribution from initial forces, shown in Eq.(43), will

be used in the stability analysis of the elastic system in the absence of damping (Iesan 1989) [15].

$$U = k_1\Delta_1^2 + \frac{1}{2}k_2\Delta_2^2 + k_3\Delta_3^2 + 2f_1^0\Delta_1 + f_2^0\Delta_2 + 2f_3^0\Delta_3 + \frac{(f_1^0)^2}{k_1} + \frac{(f_2^0)^2}{2k_2} + \frac{(f_3^0)^2}{k_3} \quad (43)$$

Here h is half of the vertical distance (the length of the line cd) between the two hinges. We can also see that the relation between the generalized coordinates and displacements at point a and b is

$$u_a = h \tan \phi - h \tan(\phi - \beta), \quad (44)$$

$$u_b = h \tan \theta - h \tan(\theta - \alpha). \quad (45)$$

Newton's second law for the mass points a and b gives the following equations of motion in terms of the generalized coordinates $\alpha(t)$ and $\beta(t)$, and the displacements $u_a(t)$ and $u_b(t)$.

$$m_a \ddot{u}_a = P_a + f_2 + 2f_3 \sin(\phi - \beta), \quad (46)$$

$$m_b \ddot{u}_b = 2f_1 \sin(\theta - \alpha) - f_2. \quad (47)$$

where f_1 , f_2 , and f_3 are the internal forces in the k_1 , k_2 , and k_3 springs, respectively, and m_a and m_b are the masses at points a and b , respectively. Effects of masses have been discussed in References [46] and [47]. By substituting the kinematic relations, Eqs.(44) and (45), into Eqs.(46) and (47), the equations of motion can be expressed in terms of the generalized coordinates:

$$\mathbf{A} \begin{pmatrix} \ddot{\alpha} \\ \ddot{\beta} \end{pmatrix} + \mathbf{B} \begin{pmatrix} \dot{\alpha}^2 \\ \dot{\beta}^2 \end{pmatrix} = \begin{pmatrix} 2f_1(t) \sin(\theta - \alpha) - f_2(t) \\ P_a + f_2(t) + 2f_3(t) \sin(\theta - \beta) \end{pmatrix}, \quad (48)$$

where

$$\mathbf{A} = \begin{bmatrix} m_b h \sec^2(\theta - \alpha) & 0 \\ 0 & m_a h \sec^2(\phi - \beta) \end{bmatrix}, \quad (49)$$

$$\mathbf{B} = \begin{bmatrix} -2m_b h \sec^2(\theta - \alpha) \tan(\theta - \alpha) & 0 \\ 0 & -2m_a h \sec^2(\phi - \beta) \tan(\phi - \beta) \end{bmatrix}, \quad (50)$$

Hooke's law holds for linearly elastic springs and the relation between force and deformation is linear, that is,

$$f_1 = k_1\Delta_1 + f_1^0, \quad (51)$$

$$f_2 = k_2\Delta_2 + f_2^0, \quad (52)$$

$$f_3 = k_3\Delta_3 + f_3^0, \quad (53)$$

where the f 's are the total spring forces, and f^0 's are the initial forces or pre-loads inside the springs. The sign convention of the internal forces is chosen so that tension is positive. If we substitute the constitutive equations into the equations of motion, we obtain the governing equations in the generalized coordinates:

$$\mathbf{A} \begin{pmatrix} \ddot{\alpha} \\ \ddot{\beta} \end{pmatrix} + \mathbf{B} \begin{pmatrix} \dot{\alpha}^2 \\ \dot{\beta}^2 \end{pmatrix} = \begin{pmatrix} G_1 \\ G_2 \end{pmatrix}. \quad (54)$$

$$G_1 = \frac{2k_1 h \sin(\theta - \alpha)}{\cos(\theta - \alpha)} - \frac{2k_1 h \sin(\theta - \alpha)}{\cos \theta} + 2f_1^0 \sin(\theta - \alpha) - [k_2(h \tan(\phi - \beta) - h \tan(\theta - \alpha) - h \tan \phi + h \tan \theta) + f_2^0]. \quad (55)$$

$$G_2 = P_a + [k_2(h \tan(\phi - \beta) - h \tan(\theta - \alpha) - h \tan \phi + h \tan \theta) + f_2^0] + \frac{2k_3 h \sin(\phi - \beta)}{\cos(\phi - \beta)} - \frac{2k_3 h \sin(\phi - \beta)}{\cos \phi} + 2f_3^0 \sin(\phi - \beta). \quad (56)$$

If we assume quasi-static processes, the right hand side of Eq. (54) is zero. Then Eq.(54) can be restated as the following equilibrium equations. The strategy used here is analogous to Eqs. (61) and (62) in the previously mentioned linear model, and the purpose is to relate the two generalized coordinates to the only applied load at point a .

$$\beta = \phi - \arctan(\tan \phi - \tan \theta + \tan(\theta - \alpha) - \frac{f_2^0}{k_2 h} + 2\frac{k_1}{k_2}(\frac{-\sin(\theta - \alpha)}{\cos \theta} + \tan(\theta - \alpha) + \frac{f_1^0}{k_1 h} \sin(\theta - \alpha))) \quad (57)$$

$$P_a = -[k_2 h(\tan(\phi - \beta) - \tan(\theta - \alpha) + \tan \theta - \tan \phi) + f_2^0] - 2[\frac{k_3 h}{\cos(\phi - \beta)} - \frac{k_3 h}{\cos \phi} + f_3^0] \sin(\phi - \beta). \quad (58)$$

The equilibrium equations (57) and (58) are responsible for generating load-displacement curves with no restriction on the magnitude of the displacements at nodes a and b .

The above problem can be linearized as follows, in the absence of pre-load, The purpose of using a linearized formulation is to make a comparison with the geometrical nonlinear analysis. The analysis is conducted using the energy method under the quasi-static assumption, that is, neglecting inertial terms. The total strain energy of the system is, in terms of the displacements u_a and u_b ,

$$U = 2U_1 + U_2 + 2U_3, \quad (59)$$

where $U_1 = k_1(x_b \sin \theta)^2$, $U_2 = k_2(x_b - x_a)^2$, and $U_3 = k_3(x_a \sin \phi)^2$. Here θ and ϕ are the angles of springs bc and ac from the vertical line, bd , indicating the initial configuration of the system. The subscripts 1, 2, and 3 denote the bc or bd spring, ab spring, and the ac or ad spring, respectively. In other words, the subscripts 1, 2, and 3 represent the springs with the spring constant, k_1 , k_2 , and k_3 , respectively. We now obtain the force displacement relation for the spring system. We can do so by a direct application of Newton's second law or by an energy method such as Castigliano's (first) principle (Fung 1968) [11], which states that for linear elastic materials under small deformation, the partial derivative of the total strain energy with respect to an external force is equal to the displacement in the structure corresponding to that force. Specifically, $P_i = \partial U(x_j)/\partial x_i$, where i and j denote the generalized coordinates. The force-displacement relation for the system is

$$\begin{bmatrix} k_2 + 2k_3 \sin^2 \phi & -k_2 \\ k_2 & k_2 + 2k_1 \sin^2 \theta \end{bmatrix} \begin{pmatrix} u_a \\ u_b \end{pmatrix} = \begin{pmatrix} P_a \\ P_b \end{pmatrix}. \quad (60)$$

We can use Eq.(60) and the pre-determined parameters of stiffness and initial geometry of the system to obtain a specific load-displacement relation of the system. With the assumption that the force $P_b = 0$, the degrees of freedom of the system can be reduced from two to one. Equations (61) and (62) show explicitly the interrelation between the two degrees of freedom and the load-displacement relation at point a , respectively:

$$u_b = \frac{k_2}{k_2 + 2k_1 \sin^2 \theta} u_a, \quad (61)$$

$$u_a = \frac{k_2 + 2k_1 \sin^2 \theta}{2k_2 k_3 \sin^2 \phi + 2k_1 k_2 \sin^2 \theta + 4k_1 k_3 \sin^2 \phi \sin^2 \theta} P_a. \quad (62)$$

The ratio of P_a to u_a in Eq.(62) can be considered as the effective stiffness of the linearized system in the incremental sense. Equations (61) and (62) will be used to compare with the following analysis which incorporates the effects of pre-load in a full nonlinear representation. Observe that as we might expect, all terms are positive and there are no singularities.

In the following numerical calculations of the spring system in Figure 4, we assume $h = \sqrt{10}$ mm, $\theta = 30^\circ$, and $\phi = 60^\circ$ as initial conditions. Pre-load in the spring k_2 will modify this geometry in the absence of an external force. Figure 4 shows the static characteristics of the mechanical spring system without the k_3 springs, based on Eqs.(44) and (45) for u_a and u_b and Eq. (58) for P_a in terms of the generalized coordinates, angles α and β . For $k_3 = 0$ in Figure 4, the system is equivalent to a series (Reuss) composite cell. We remark that Lakes and Drugan (2002) [25] showed that this type of system is unstable if it is unconstrained. Geometrical nonlinearity is manifest in the calculation to include the effect of the change of

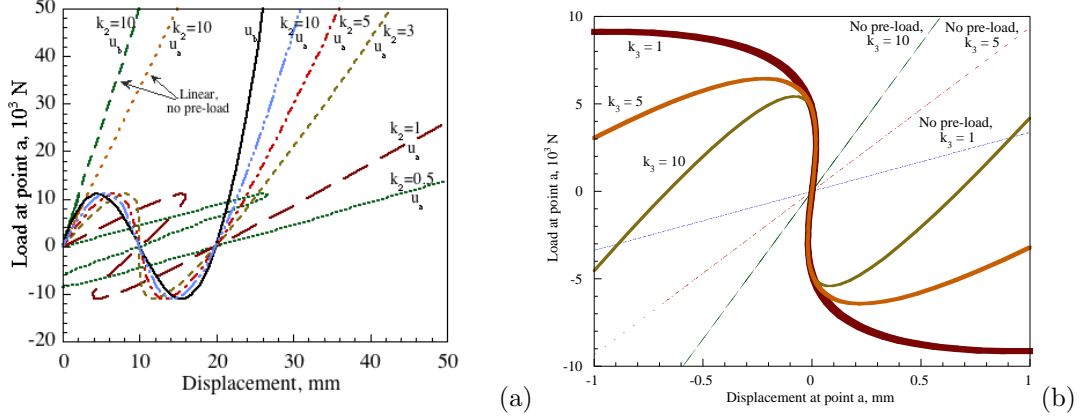


Figure 5: (a) Load-displacement diagram for the spring system in Figure 4(a) with no k_3 springs and no initial forces. (b) The load-displacement diagram for the spring system in Figure 4(b) with pre-load [44].

structural shape, even though each spring has a linear force-deformation characteristic, because the angles change as the system is deformed. In the linear approximation, the system will never buckle due to the lack of consideration of geometrical changes, as the straight lines (see Figure 5, labeled with ‘no pre-load’). The match of the slopes of the load-displacement curves for the linear and geometrical nonlinear analysis near zero deformation confirms the validity of our calculation. By tuning the stiffness of the k_2 springs, it can be seen that the overall stiffness of the system at point a , the loading point, approaches infinity around $u_a = 10$ mm when $k_1 = 10$ and $k_2 = 3$ kN/m. If we observe the curves for $k_2 < 3$ kN/m, it is understood that the corresponding functions for the curves are multi-valued functions with respect to both displacement and loads. The snap-through or back-through phenomena in both the numerical simulations by solving Eq.(46) and (47) with the Newton-Raphson method (Bathe 1996) [1] for nonlinear equations and the laboratory experiments will occur if one tries to control either the displacement or the loading at point a . However, in this case, by controlling the generalized coordinate α by hand, the curves can be numerically constructed with a one-to-one relation between α and the linear displacement u_a , and α and the loading P_a through Eq.(57) and (58).

It is understood that each of the initial forces, f_1^0 , f_2^0 , and f_3^0 , is a free parameter: there are no equations relating them. If we specify the initial forces, the spring forces f_1 , f_2 , and f_3 will change, and the geometry of the system will also change. A nonzero f_2^0 as chosen here causes the geometry of the system to change accordingly. The same effect also could be obtained by changing the initial configuration of the system, that is, adjusting θ and ϕ directly, with nonzero initial forces inside all the springs.

For purely elastic cases, we can investigate the stability of the critical equilibrium position of the spring model in Figure 4 by the energy method. Equation (43) is plotted as a surface in Figure 6 with respect to the displacements at points a and b . The parameters are $k_1 = 10$, $k_2 = 3$, $k_3 = 5$ kN/m, $f_1^0 = 0$, $f_2^0 = -30$ N, $f_3^0 = 0$, $\theta = 30$, and $\phi = 60$. The magnitude of the masses m_1 and m_2 is irrelevant to the calculation because of the quasi-static assumption.

In Figure 6(a), it can be seen that the surface has a saddle shape at the critical equilibrium point, $u_a = 0$ mm and $u_b = 10$ mm. As a comparison, Figure 6(b) shows the energy profile of the solid-solid phase transition of BaTiO₃, based on the Landau phenomenological theory. The concave-down energy curve indicates negative stiffness. It is understood that the system is not stable at the saddle point. The system is not necessarily free to have any values of the coordinates u_a and u_b ; it is constrained by the equilibrium equations. For example applying Eq.(57) gives a concave-up section of the saddle, which suggests stability in the presence of perturbations in the force P_a . However, the application of Eq.(58) with $P_a = 0$ gives a concave down section of the saddle surface in Figure 6, indicating instability in the presence of perturbations of P_b . Both

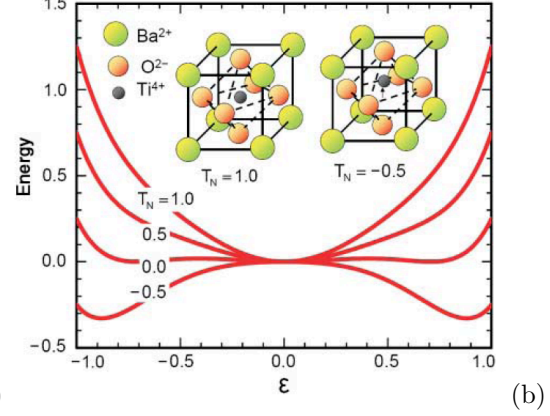
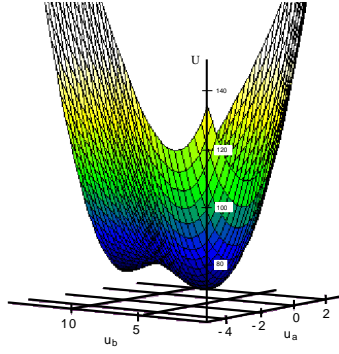


Figure 6: (a) Two-dimensional energy landscape of the spring model in Figure 4 with respect to u_a and u_b with no force at point a or b . $k_1 = 10$, $k_2 = 3$, $k_3 = 5$ kN/m, $f_1^0 = 0$, $f_2^0 = -30$ N, and $f_3^0 = 0$ [44]. (b) Energy landscape of the barium titanate before and after phase transition [16].

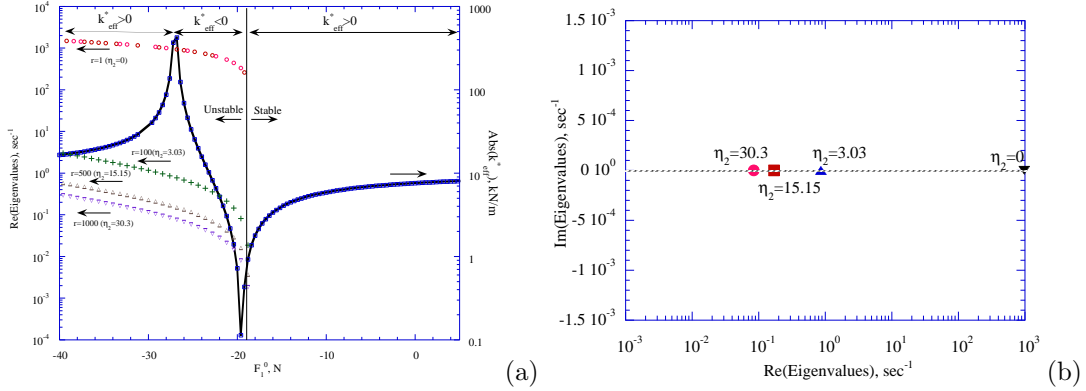


Figure 7: (a) Effective stiffness and the stability-losing eigenvalue vs. pre-stress (F_1^0). (b) Root-locus plot of the system with $F_1^0 = -27.2$, $F_2^0 = 0$, and $F_3^0 = 0$ N. The tuning parameter is η , the viscous element parallel to the k_2 spring [44].

degrees of freedom must be considered in an energy approach to determine the stability of this system.

As shown in Figure 7, the magnitude of the stability-losing eigenvalue decreases with the increase of viscosity. This can be clearly seen on the root-locus plot, as shown in Figure 7(b). Moreover, we remark that the inverse of the eigenvalue is the divergence rate associated with instability. Therefore, the system is metastable at the equilibrium configuration with extreme high overall stiffness. The rate of divergence from equilibrium becomes slower as the viscosity η is increased. Near the stability boundary, in the stable regime, the system exhibits extreme high overall compliance around $F_1^0 = -19$ N.

7 Some remarks on related issues and real-world applications

7.1 Negative stiffness vs. negative Poisson's ratio (or called auxetic materials)

Negative stiffness is to be distinguished from a negative Poisson ratio [21]. Poisson's ratio, denoted as ν , is defined as the negative lateral strain of a stressed body divided by its longitudinal strain. Based on the assumption of positive definiteness of the strain energy for isotropic and homogeneous solids, ν ranges from -1 to 0.5, which implies stability. Positive definiteness does not specify the particular value of Poisson's ratio within that range. The value of ν for most solid materials is between 0.25 and 0.33. Recently, foams with ν as small as -0.8 have been made and analyzed [21]. When ν is negative, materials become fatter in cross section when they are stretched. The stiffness of these foams is nevertheless positive.

7.2 Negative stiffness does not violate thermodynamic laws

The negative stiffness is obtainable through different processes. In structural mechanics, negative stiffness is obtainable through post-buckling processes, which is a structural effect. Buckling induced negative stiffness has been known in the computational mechanics community for a long time. In solid materials, the Landau phenomenological theory on phase transformation predicts negative curvature in system free energy, i.e. negative stiffness, in the vicinity of phase transitions.

In the context of thermodynamics, compressibility must be positive. This contradicts the above result of elasticity theory. A continuum has an infinite number of degrees of freedom, while a solid made of finite, and hence a finite number of degrees of freedom. Thermodynamics suggests metastability in Van der Waals fluids due to negative compressibility. The non-monotonic portion of the pressure-volume relation is strongly related to negative stiffness. Therefore the condition of a passive material with positive damping in this case does not contradict the elasticity result that a fully constrained object with $K < 0$ or $E < 0$ can be stable. Negative stiffness does not violate laws of equilibrium or non-equilibrium thermodynamics in the sense that stability is achieved by surrounding environments [39] [26]. In this view, the behavior of the inclusion in the composite is dynamic. Composites with passive or dynamic inclusions may behavior completely different [17].

7.3 Negative stiffness vs. negative permittivity

The causal mechanism for the phenomena due to negative stiffness inclusions is the balance between the contributions from negative stiffness and positive stiffness phases. This gives rise to amplified motion at the interface between constituents. One must emphasize that although response curves resemble resonance, the causal mechanism does not entail any inertial terms, in contrast to resonant effects in which extreme characteristics can be seen with a dilute concentration of heterogeneities (Nicolovici *et al.* 1994) [34] and in contrast with dielectric systems which attain negative permittivity near a resonance (Bergman and Stroud 1992) [3]. Along this line of research, many successful progresses have been made in recent years for the development of metamaterials (see the review article [5]).

7.4 Real-world applications

The original intention of using negative stiffness in composite materials is to obtain high damping and high stiffness simultaneously, which has important applications in vibration isolation as required in earthquake

engineering, high-speed trains, semiconductor factories and car bumpers. The NS composite materials have been developed for this purpose albeit in a metastable state [17]. In addition, as in thermoelastic and piezoelectric materials, elasticity is coupled with temperature and electric field respectively, these composites may be used in high-performance sensors and actuators [43]. Furthermore, these composites may also occur naturally in rocks and in biological materials; they may be considered in the context of deep-focus earthquakes and attenuation of seismic waves [24].

8 Conclusions and outlook

Negative stiffness is not illegal. It is just unstable. However, it can be stabilized by positive-stiffness surroundings. The sources of negative stiffness are pre-load, geometric nonlinear effects or phase transitions (which can be viewed as geometric nonlinearity at the atomic scales). For the pre-load, an analogy can be made in the field of dislocations for crystalline materials. The extreme effective elastic, viscoelastic, thermoelastic, pyroelastic and piezoelectric properties of composite materials (discrete or continuous), that are results of negative stiffness, may be found valuable in the future.

The first paper published on using negative stiffness to achieve extreme viscoelastic properties of solid materials was 10 years ago. This year makes the 10th anniversary for the discovery. Many important progresses have been made at the theoretical end [7], [18], [48], [49] and at the application end [17], [9]. There are still many open questions in the field to be clarified.

9 Acknowledgments

The author is grateful for funding from the Taiwan National Science Council under the contract number NSC 98-2221-E-006-131-MY3.

References

- [1] K. J. Bathe, *Finite Element Procedures*, Prentice Hall, Englewood Cliffs, NJ (1996)
- [2] R. Bellman, *Stability Theory of Differential Equations*, McGraw-Hill, New York, NY (1953)
- [3] D. J. Bergman and D. Stroud, Physical properties of macroscopically inhomogeneous media, *Solid State Physics* 46, 147-269 (1992)
- [4] J. H. Bramble and L. E. Payne, On the uniqueness problem in the second boundary value problem in elasticity, *Proceedings of the U.S. Fourth National Congress of Applied Mechanics*, pp. 469-473 (1963)
- [5] H. Chen, C. T. Chan, P. Sheng, transformation optics and metamaterials, *Nature Materials* 9, 387-396 (2010)
- [6] R. M. Christensen, *Theory of Viscoelasticity*, 2nd Ed., Dover Publication, Mineola, New York, NY (1982)
- [7] W.J. Drugan, Elastic Composite Materials Having a Negative Stiffness Phase Can Be Stable, *Physical Review Letters* 98, 055502 (2007)
- [8] R. C. Dorf, *Stability Problems in Fracture Mechanics*, John Wiley & Sons, New York, NY (1992)

- [9] A. D. Fortes E. Suard, K. S. Knight, Negative Linear Compressibility and Massive Anisotropic Thermal Expansion in Methanol Monohydrate, *Science* 331, 742-746 (2011)
- [10] F. Falk, Model free energy, mechanics, and thermodynamics of shape memory alloys, *Acta Metall.* 285, 1773-1780 (1980)
- [11] Y. C. Fung, *Foundations of solid mechanics*, Prentice-Hall, Englewood, NJ (1968)
- [12] P. Gallina, About the stability of non-conservative undamped systems, *Journal of Sound and Vibration*, 262, 977-988 (2003)
- [13] Z. Hashin and S. Shtrikman, A variational approach to the theory of the elastic behavior of multiphase materials. *Journal of the Mechanics and Physics of Solids* 11, 127-140 (1963)
- [14] H. H. Huang, C. T. Sun, G. L. Huang, On the negative effective mass density in acoustic metamaterials, *International Journal of Engineering Science* 47, 610-617 (2009)
- [15] D. Iesan, *Prestressed Bodies*, Addison-Wesley, Longman, England (1989)
- [16] T. Jaglinski, D. Kochmann, D. Stone, R.S. Lakes, Composite materials with viscoelastic stiffness greater than diamond, *Science* 315, 620-622 (2007)
- [17] T. Jaglinski, R.S. Lakes, Zn-Al based metal matrix composites with high stiffness and high viscoelastic damping, *Journal of Composite Materials*, in press (2011)
- [18] D.M. Kochmann, W.J. Drugan, Dynamic stability analysis of an elastic composite material having a negative-stiffness phase, *Journal of the Mechanics and Physics of Solids* 57, 1122-1138 (2009)
- [19] J. K. Knowles and E. Sternberg, On the failure of ellipticity and the emergence of discontinuous gradients in plane finite elastostatics, *Journal of Elasticity* 8, 329-379 (1978)
- [20] R. J. Knops and E. W. Wilkes, Theory of elastic stability, *Handbuch der physik*, VIa/1-4, S. Flugge Ed., Springer-Verlag, Berlin (1973)
- [21] R. S. Lakes, Advances in negative Poisson's ratio materials, *Advanced Materials* 5. 293-296 (1993)
- [22] R. S. Lakes, Extreme damping in compliant composites with a negative-stiffness phase, *Philosophical Magazine Letters* 81, 95-100. (2001)
- [23] R. S. Lakes, Extreme damping in composite materials with a negative stiffness phase, *Physical Review Letters*, 86, 2897-2900 (2001)
- [24] R.S. Lakes, T. Lee, A. Bersie, Y.C. Wang, Extreme damping in composite materials with negative-stiffness inclusions, *Nature* 410, 565-567 (2001)
- [25] R. S. Lakes and W. J. Drugan, Dramatically stiffer elastic composite materials due to a negative stiffness phase?, *Journal of the Mechanics and Physics of Solids*, 50, 979-1009 (2002)
- [26] R. Lakes and K. W. Wojciechowski, Negative compressibility, negative Poissons ratio, and stability, *Physica status solidi (b)* 245, 545-551 (2008)
- [27] H. Leipholz, *Stability of elastic systems*, Sijthoff & Noordhoff, Alphen aan den Rijn, The Netherlands, 1980.
- [28] H. Leipholz, *Stability theory : an introduction to the stability of dynamic systems and rigid bodies*, 2nd Ed., B. G. Teubner GmbH, Germany (1987)
- [29] A. M. Lyapunov, *The general problem of the stability of motion*, CRC Press (1992)
- [30] J. E. Marsden and T. S. Ratiu, *Introduction to Mechanics and Symmetry*, Springer-Verlag, New York, NY (1994)

- [31] L. Meirovitch, *Methods of Analytical Dynamics*, McGraw-Hill, New York (1970)
- [32] D. R. Merkin, *Introduction to the Theory of Stability*, Springer-Verlag, New York, NY (1997)
- [33] G. W. Milton, Modelling the properties of composites by laminates, In *Homogenization and Effective Moduli of Materials and Media*, J.L. Erickson, D. Kinderlehrer, R. Kohn and J. L. Lions (eds). Springer Verlag: Berlin, 1986; 150–175.
- [34] N. A. Nicorovici and R. C. McPhedran and G. W. Milton, Optical and dielectric properties of partially resonant systems, *Physical Review B* 49, 8479-8482 (1994)
- [35] B. Paul, Prediction of elastic constants of multiphase materials, *Trans. AIME* 1960; **218**:36–41.
- [36] G. Puglisi and L. Truskinovsky, Mechanics of a discrete chain with bi-stable elements, *J. Mech. Phys. Solids* 48, 1- 27 (2000)
- [37] P. Rosakis and A. Ruina and R. S. Lakes, Microbuckling instability in elastomeric cellular solids, *J. Materials Science* 28, 4667-4672 (1993)
- [38] E. Salje, *Phase transitions in ferroelastic and co-elastic crystals*, Cambridge University Press, Cambridge, London (1990)
- [39] X. Shang, and R.S. Lakes, Stability of elastic material with negative stiffness and negative Poisson's ratio, *Physica status solidi (b)* 244, 1008-1026 (2007)
- [40] I. Stewart, *Does God Play Dice?: The New Mathematics of Chaos*, Viking Penguin, New York, NY (1997)
- [41] S. H. Strogatz, *Nonlinear Dynamics and Chaos*, Perseus Books, Cambridge, Massachusetts (1994)
- [42] S. P. Timoshenko and J. N. Goodier, *Theory of Elasticity* (3rd edn), McGraw-Hill, New York, NY (1970)
- [43] Y. C. Wang and R. S. Lakes, Extreme thermal expansion, piezoelectricity, and other coupled field properties in composites with a negative stiffness phase, *J. Appl. Phys.* 90, 6458-6465 (2001)
- [44] Y.C. Wang, R.S. Lakes, Extreme stiffness systems due to negative stiffness elements, *American Journal of Physics* 72, 40-50. (2004)
- [45] Y. C. Wang and R. Lakes, Stability of negative stiffness viscoelastic systems, *Quarterly of Applied Mathematics* 63, 34-55 (2005)
- [46] Y.C. Wang, Influences of negative stiffness on a two-dimensional hexagonal lattice cell, *Philosophical Magazine* 87, 3671-3688 (2007)
- [47] Y. C. Wang, J. G. Swadener, R. S. Lakes, Anomalies in stiffness and damping of a 2D discrete viscoelastic system due to negative stiffness components, *Thin Solid Films* 515, 3171-3178 (2007)
- [48] Y.C. Wang and C.C. Ko, Stress analysis of a two-phase composite having a negative-stiffness inclusion in two dimensions, *Interaction and Multiscale Mechanics* 2, 321 (2009)
- [49] Y. C. Wang, C. Y. Wu and Q. Y. Kuo, Negative stiffness of a buckled carbon nanotube in composite systems via molecular dynamics simulation, *Physica status solidi (b)* 248, 88-95 (2011)